Dynamics of Endocytosis and Exocytosis of Poly(D,L-Lactide-*co*-Glycolide) Nanoparticles in Vascular Smooth Muscle Cells

Jayanth Panyam[1] and Vinod Labhasetwar[1,2,3]

Received October 3, 2002; accepted October 8, 2002

Purpose. The purpose of this work was to characterize the process of endocytosis, exocytosis, and intracellular retention of poly (D,L-lactide-*co*-glycolide) nanoparticles *in vitro* using human arterial vascular smooth muscle cells (VSMCs).

Methods. Nanoparticles containing bovine serum albumin (BSA) as a model protein and 6-coumarin as a fluorescent marker were formulated by a double emulsion-solvent evaporation technique. The endocytosis and exocytosis of nanoparticles in VSMCs were studied using confocal microscopy and their intracellular uptake and retention were determined quantitatively using high-performance liquid chromatography.

Results. Cellular uptake of nanoparticles (mean particle size 97 ± 3 nm) was a concentration-, time-, and energy-dependent endocytic process. Confocal microscopy demonstrated that nanoparticles were internalized rapidly, with nanoparticles seen inside the cells as early as within 1 min after incubation. The nanoparticle uptake increased with incubation time in the presence of nanoparticles in the medium; however, once the extracellular nanoparticle concentration gradient was removed, exocytosis of nanoparticles occurred with about 65% of the internalized fraction undergoing exocytosis in 30 min. Exocytosis of nanoparticles was slower than the exocytosis of a fluid phase marker, Lucifer yellow. Furthermore, the exocytosis of nanoparticles was reduced after the treatment of cells with the combination of sodium azide and deoxyglucose, suggesting that exocytosis of nanoparticles is an energy-dependent process. The nanoparticle retention increased with increasing nanoparticle dose in the medium but the effect was relatively less significant with the increase in incubation time. Interestingly, the exocytosis of nanoparticles was almost completely inhibited when the medium was depleted of serum. Further studies suggest that the addition of BSA in the serum free medium with or without platelet derived growth factor (PDGF) induced exocytosis of nanoparticles. The above result suggests that the protein in the medium is either adsorbed onto nanoparticles and/or carried along with nanoparticles inside the cells, which probably interacts with the exocytic pathway and leads to greater exocytosis of nanoparticles.

Conclusions. The study demonstrated that endocytosis and exocytosis of nanoparticles are dynamic and energy-dependent processes. Better understanding of the mechanisms of endocytosis and exocytosis, studies determining the effect of nanoparticle formulation and composition that may affect both the processes, and characterization of intracellular distribution of nanoparticles with surface modifications would be useful in exploring nanoparticles for intracellular delivery of therapeutic agents.

KEY WORDS: cytoplasmic delivery; endo-lysosomal escape; sustained release; intracellular uptake; sustained retention.

INTRODUCTION

The formulation of macromolecular agents, such as proteins, oligonucleotides, and DNA, in drug-delivery systems is being widely investigated because of the increased interest in their use as therapeutics (1–3). Most of these therapeutic agents require intracellular uptake for their therapeutic effect because their site of action is within the cell. However, the major limitation with macromolecular therapeutics is their inefficient intracellular uptake and susceptibility to degradation during uptake by endocytosis (4).

Various carriers or vectors have been used for the efficient intracellular delivery of different classes of macromolecular therapeutics. Viral systems, such as adenovirus, adenoassociated virus, or influenza virus, and nonviral systems, such as cationic lipids, cationic polymers, or dendrimers, have been used for delivering DNA and/or antisense oligonucleotides (1). Intracellular delivery of proteins has been performed by attaching them through covalent or noncovalent links to protein transduction domains capable of entering the cell without the necessity of going through the endocytic pathways (3). However, all these systems are limited by their ability to carry only certain types of cargoes and some of these systems (e.g., viral vectors) are limited by concerns of toxicity and immunogenicity.

We have previously shown that biodegradable nanoparticles formulated from poly (D,L-lactide-*co*-glycolide; PLGA) rapidly escape the degradative endo-lysosomal compartment and are capable of delivering a variety of payloads into the cytoplasm (5–7). PLGA is a biocompatible and biodegradable polymer and is approved by the US Food and Drug Administration for human use (8). Another advantage of PLGA nanoparticles is their ability to sustain the release of the encapsulated therapeutic agent (9). Development of PLGA nanoparticles as an efficient carrier for the intracellular drug and macromolecular delivery would depend on their efficient internalization and sustained retention inside the cell (10). However, the process of intracellular nanoparticle uptake and retention is not very well characterized. The objective of the present study was therefore to characterize the process of endocytosis and exocytosis of PLGA nanoparticles *in vitro* using human arterial vascular smooth muscles cells (VSMCs). We have selected VSMCs as a model cell line because of our interest in investigating nanoparticles for localized delivery of antiproliferative agents and genes to the arterial tissue to prevent restenosis (11,12). Restenosis is the reobstruction of a blood vessel after angioplasty or stenting, the commonly used techniques to relieve the obstruction. Proliferation and migration of VSMCs in response to a vascular injury caused by the above techniques is considered as the main factor responsible for the reobstruction of blood vessel (13). VSMCs are commonly used as a model cell line to study the antiproliferative effect of therapeutic agents *in vitro*.

MATERIALS AND METHODS

Materials

Bovine serum albumin (BSA, Fraction V), sodium azide, deoxyglucose, and polyvinyl alcohol (PVA, average molecu-

[1] Department of Pharmaceutical Sciences, University of Nebraska Medical Center, Omaha, Nebraska 68198-6025.

[2] Department of Biochemistry and Molecular Biology, University of Nebraska Medical Center, Omaha, Nebraska 68198-6025.

[3] To whom correspondence should be addressed. (e-mail: vlabhase@unmc.edu)

0724-8741/03/0200-0212/0 © 2003 Plenum Publishing Corporation

lar weight 30,000–70,000) were purchased from Sigma (St. Louis, MO, USA). LysoTracker Red®, Lucifer Yellow (lithium salt), and FM-64 cellular markers were purchased from Molecular Probes (Eugene, OR, USA). 6-coumarin was purchased from Polysciences (Warrington, PA, USA). PLGA (50:50 lactide-glycolide ratio, 143,000 Da) was purchased from Birmingham Polymers (Birmingham, AL, USA). All the reagents used for transmission electron microscopy (TEM) were from Electron Microscopy Services (Ft. Washington, PA, USA).

Methods

Nanoparticle Formulation and Characterization

Nanoparticles containing BSA as a model macromolecule and 6-coumarin as a fluorescent marker were formulated using a double emulsion-solvent evaporation technique as described previously (14). In brief, an aqueous solution of BSA (60 mg/mL) was emulsified in a polymer solution (180 mg in 6 mL of chloroform) containing 6-coumarin (100 μg) using a probe sonicator (55 Watts for 2 min; Sonicator® XL, Misonix, NY, USA). The water-in-oil emulsion thus formed was further emulsified into 50 mL of 2.5% w/v aqueous solution of PVA by sonication as above for 5 min to form a multiple water-in-oil-in-water emulsion. The multiple emulsion was stirred for ~18 h at room temperature followed by for 1 h in a desiccator under vacuum. Nanoparticles thus formed were recovered by ultracentrifugation (100,000 g for 20 min at 4°C, Optima™ LE-80K, Beckman, Palo Alta, CA, USA), washed two times to remove PVA, unentrapped BSA, and 6-coumarin, and then lyophilized (Sentry™, Virtis, Gardiner, NY, USA) for 48 h to obtain a dry powder.

Nanoparticles were characterized for particle size by TEM. A drop of nanoparticle suspension (1 mg/mL) was placed on to the TEM grid and the particles were visualized following a negative staining with 2% uranyl acetate using a Philips 201® transmission electron microscope (Philips/FEI Inc., Briarcliff Manor, NY, USA). Zeta potential (surface charge) of nanoparticles (0.5 mg/mL in water) was determined using Zeta Plus™ zeta potential analyzer (Brookhaven Instruments Corp., Holtsville, NY, USA).

Cell Culture

Human vascular smooth muscle cells (VSMCs, Cascade Biologics, Portland, OR, USA) were maintained on Medium 231 supplemented with smooth muscle growth supplement (Cascade Biologics) and 100 μg/mL penicillin G and 100 μg/mL streptomycin (Gibco BRL, Grand Island, NY, USA). For studies with serum-free media, Medium 231 without the added growth supplement was used.

Cellular Nanoparticle Uptake Studies

VSMCs were seeded at 50,000 cells/mL/well in 24-well plates (Falcon®, Becton Dickinson) and allowed to attach for 24 h. To determine the nanoparticle uptake, cells were incubated with a nanoparticle suspension in growth medium, washed three times with phosphate-buffered saline (PBS, pH 7.4, 154 mM) and then lysed by incubating them with 0.1 mL of 1× cell culture lysis reagent (Promega, Madison, WI, USA) for 30 min at 37°C. The cell lysates were processed to determine the nanoparticle levels by high-performance liquid chromatography (HPLC) as per our previously published method (15). Results were expressed as nanoparticle amount in μg per mg total cell protein.

Initially, the dose- and time-dependent cellular uptake of nanoparticles was determined. To study the dose-dependent nanoparticle uptake, cells were incubated with different concentrations of nanoparticle suspension (10–1000 μg/mL) for 1 h. To study the time-dependent nanoparticle uptake, cells were incubated with a suspension of nanoparticles (100 μg/mL) for different time periods. Exocytosis of nanoparticles was followed by incubating the cells with nanoparticles (100 or 200 μg/mL) for either 1 or 3 h in either regular growth medium or in serum-free medium (SFM), followed by washing off of the uninternalized nanoparticles with PBS for two times. The intracellular nanoparticle level after the washing of the cells was taken as the zero time point value. The cells in other wells were then incubated with fresh growth medium. At different time intervals, the medium was removed, cells were washed twice with PBS and lysed, and the intracellular nanoparticle levels were analyzed to obtain the fraction of nanoparticles that were retained. To determine the mass balance, nanoparticle fraction that exocytosed into the medium was also analyzed for each time point.

To study the effect of metabolic inhibition on nanoparticle exocytosis, VSMCs were incubated with nanoparticles (100 μg/mL) for 1 h in regular growth medium as before, followed by washing off of the uninternalized particles with PBS for two times. This was followed by incubation of cells in regular growth medium containing 0.1% w/v sodium azide and 50 mM of deoxyglucose, and exocytosis was followed as before. To study the exocytosis of a fluid phase marker, Lucifer yellow, VSMCs were incubated with 100 μg/mL of Lucifer yellow for 1 h followed by washing with PBS and lysing of cells as described above for nanoparticles. Lucifer yellow levels in the cell lysate were measured by spectrofluorometry (λ_{ex} 465 nm and λ_{em} 535 nm).

Microscopic Studies

For confocal laser scanning microscopy, VSMCs were plated 24 h before the experiment in Bioptech® plates (Bioptechs, Butler, PA, USA) at 50,000 cells/plate in 1 mL of growth medium. The Bioptech® plate was then placed on the stage (maintained at 37°C) of the confocal microscope (Zeiss Confocal LSM410 equipped with Argon-Krypton laser, Carl Zeiss Microimaging, Inc., Thornwood, NY, USA). A representative cell was selected at random and zero-time point picture was taken in FITC and RITC filters. A 10-μL nanoparticle suspension (10 mg/mL) was then added into the medium on top of the region containing the selected cell and a series of time scans (at 10 s intervals initially and then at 1-min intervals) in the dual filter mode was obtained. To follow the exocytosis of the nanoparticles from the same cell, the medium containing the nanoparticles was carefully removed from the plate, washed three times with PBS and then filled with fresh medium. All the washings were performed without removing the culture plate from the microscope stage. Another series of time scans were obtained as described before on the same cell. To study the effect of energy depletion on nanoparticle uptake, cells were pre-incubated

for 1 h with 0.1% w/v sodium azide and 50 mM 2-deoxy glucose and then with a nanoparticle suspension (100 μg/mL) in growth medium also containing 50 nM LysoTracker Red® and 0.1% w/v sodium azide and 50 mM 6-deoxy glucose for an additional 60 min. The LysoTracker Red® dye emits red fluorescence in the acidic vesicles of cells but not at the physiologic pH and, therefore, is used as a marker for late endosomes and lysosomes. The cells were washed twice with PBS and visualized with HEPES buffer (pH 8). The images captured in RITC, FITC, and differential interference contrast were overlaid to determine localization of nanoparticles in endo-lysosomal compartments using LysoTracker Red® as a marker.

RESULTS

Nanoparticle Characterization

PLGA nanoparticles were formulated with BSA as a model protein and 6-coumarin as a fluorescent marker with a mean diameter of 97 ± 3 nm (mean ± SEM, average of 150 nanoparticles counted from 5 to 7 TEM fields). Nanoparticles were negatively charged with zeta potential of –20 ± 1 mV (mean ± SEM, n = 5). The fluorescent marker incorporated in the nanoparticles (~0.05% w/w loading) is lipophilic and remains associated with the polymer matrix of nanoparticles. The dye does not leach from the nanoparticles during the experimental time frame and therefore the fluorescence seen in the cells is caused by nanoparticles and not by the free dye. Thus, the dye incorporated in nanoparticles serves as a sensitive marker to quantitatively determine cellular uptake of nanoparticles and also to study their intracellular/tissue distribution by confocal microscopy (14). To further confirm that the dye does not leach out during the time of the experiment, nanoparticles were incubated with cell culture medium for 1 h at 37°C, centrifuged at 20,000 g for 15 min, supernatant filtered through a 0.1-μm syringe filter (Anotop™, Whatman, Clifton, NJ, USA) and the filtrate was added into the medium. Confocal microscopy showed no fluorescence inside the cells (Fig. 1A), confirming that the fluorescence seen inside the cells after nanoparticle incubation is caused by the uptake of nanoparticles and not the free dye (Fig. 1B).

Nanoparticle Uptake

Confocal microscopy of VSMCs indicated that nanoparticle uptake was inhibited in the presence of metabolic inhibitors, sodium azide and deoxy glucose (Fig. 1C compared with positive control in Fig. 1B), suggesting an endocytic process. Further characterization of the nanoparticle uptake revealed that nanoparticle uptake was both concentration- and time-dependent (Fig. 2A and B). The uptake was linear at lower doses of nanoparticles (10 to 100 μg), but the efficiency of uptake was reduced at higher doses (500–1000 μg). The nanoparticle uptake was relatively rapid during the first 2 h of incubation before reaching a saturation uptake rate in 4–6 h.

To follow the dynamics of intracellular uptake of nanoparticles, we took a series of rapid scans in the FITC and RITC filter modes after adding nanoparticles to a live cell (Fig. 3). A series of z-sections were performed at the zero time point to measure the thickness of the cell and each photograph shown is a z-section through the middle of the cell and hence the fluorescence seen is caused by the nanoparticles localized inside the cell and not on the surface. The nanoparticles were internalized rapidly and could be seen inside the cells as early as 10–30 s after incubation. Since the nanoparticles were added as a concentrated stock suspension on the top of the cell in the medium, the background fluorescence appears to be increasing as the particles are dispersing in the medium.

Exocytosis and Intracellular Retention

Confocal microscopy and quantitative analysis of nanoparticle levels were used to follow exocytosis of nanoparticles. In confocal microscopy, exocytosis of nanoparticles was followed in the same cell that was used to follow endocytosis (Fig. 4). Exocytosis started immediately after the removal of nanoparticles in the external media. Particles appeared to exocytose more from a particular region in the cell (the area pointed by arrow in Fig. 4) suggesting the possibility of a compartment within the cell from where they were being exocytosed more rapidly.

The change in fluorescence intensity of the cell images from confocal microscopy (Fig. 4) was measured using the confocal software (LSM-PC), and was found to drop to about

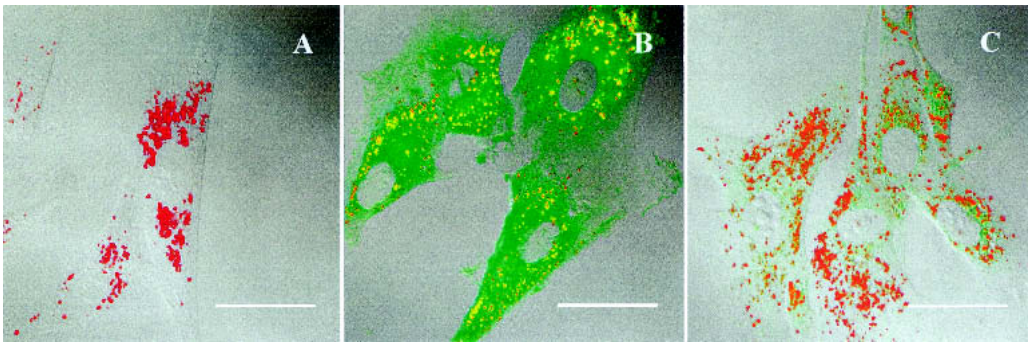

Fig. 1. Confocal microscopic images (100×) of vascular smooth muscle cells incubated with (A) medium that was preincubated with nanoparticles, centrifuged and filtered, (B) nanoparticles, and (C) nanoparticles in the presence of sodium azide and deoxyglucose. Nanoparticle fluorescence is green, the overlap of nanoparticle and LysoTracker® fluorescence (red) is shown in yellow, and the entire image is an overlay of the differential interference contrast image of the cell. Dose of nanoparticles used was 100 μg/mL in all the cases. Bar = 25 μm.

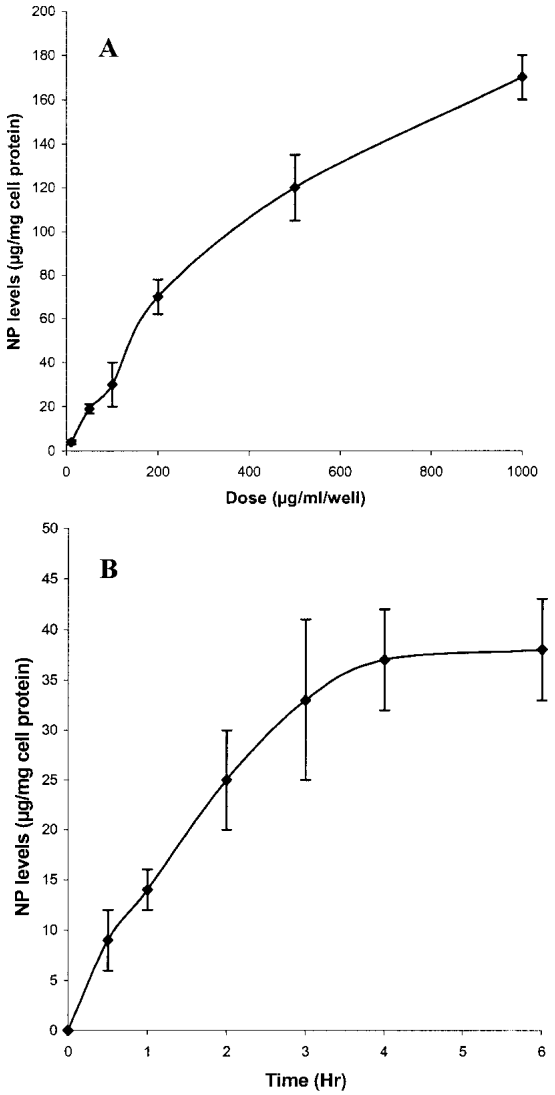

Fig. 2. Dose- (A) and time-dependent (B) uptake of nanoparticles (NP). Vascular smooth muscle cells were incubated with different doses of nanoparticles for 1 h (A) or with 100 µg/mL/well dose for different time intervals (B). Data as mean ± SEM, n = 6.

75% of the 0 min time point in 10 min. Exocytosis of nanoparticles was also followed by quantitative measurement of nanoparticle retention within the cell using HPLC. After the removal of nanoparticles from the medium, about 65% of the internalized nanoparticles were exocytosed in the first 30 min (Fig. 5A). Thus, the drop in the cellular fluorescent intensity measured using the confocal software and cellular nanoparticle levels measured using HPLC seems to match.

Increasing the dose of nanoparticles from 100 to 200 µg/mL in the medium resulted in a ~2.5-fold increased retention of nanoparticles in the cells (Fig. 5A). However, the time of incubation of nanoparticles before the exocytosis study showed relatively less significant effect on the fraction of nanoparticles that was retained (Fig. 5B). To confirm that nanoparticles were actually exocytosed out from the cells, the growth medium was analyzed for the nanoparticle levels. Figure 6 demonstrates the mass balance during the nanoparticle exocytosis; the drop in intracellular nanoparticle levels closely matched with that of the appearance of the nanoparticles in

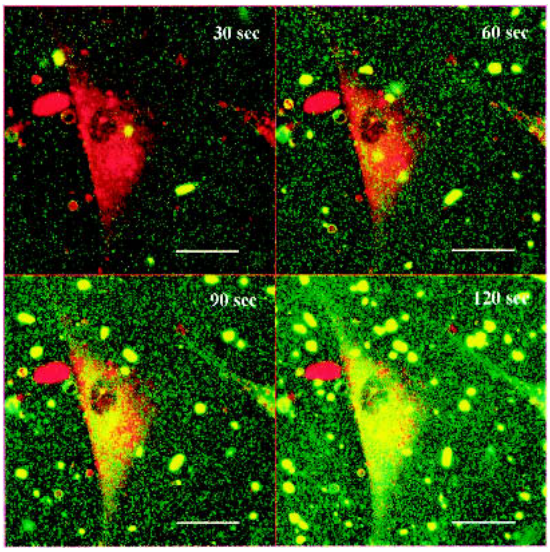

Fig. 3. Time-series confocal images (100×) of nanoparticle uptake by vascular smooth muscle cells . Cells were initially labeled with FM-64 (red fluorescence) and the nanoparticle (green fluorescence) uptake was followed by a series of time scans. The overlap of nanoparticle and FM-64 fluorescence is shown in yellow fluorescence. The dose of nanoparticles was 100 µg/mL. Large fluorescence spots seen in the background are caused by the presence of some undispersed nanoparticle aggregates. Bar = 25 µm.

the medium. Nanoparticle levels in the total cell lysate at every time point was determined and was added to the nanoparticle levels in the medium. This gave the total nanoparticle levels, which matched closely with that of intracellular nanoparticle levels at 0 h time point.

The exocytosis of PLGA nanoparticles was found to be slower and to a lower extent than that of a fluid phase marker, Lucifer yellow (Fig. 7A). The intracellular Lucifer yellow lev-

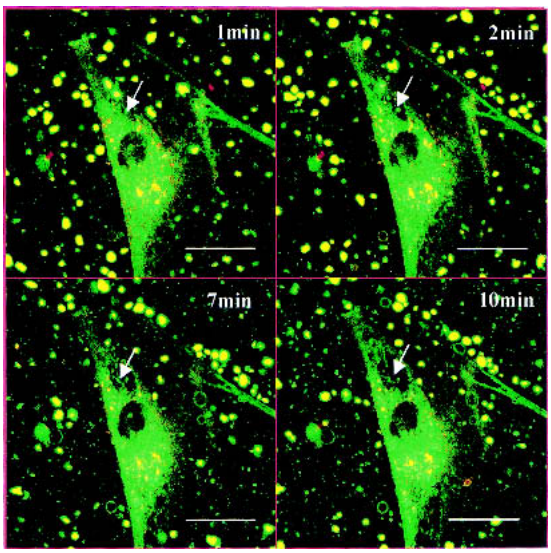

Fig. 4. Time-series confocal images (100×) of nanoparticle exocytosis. Cells were preloaded with nanoparticles (100 µg/mL) for 30 min (the cell visualized was the same used for studying endocytosis in Fig. 3) and nanoparticle exocytosis was followed by a series of time scans. Large fluorescence spots seen in the background are caused by the presence of some undispersed nanoparticle aggregates. Bar = 25 µm

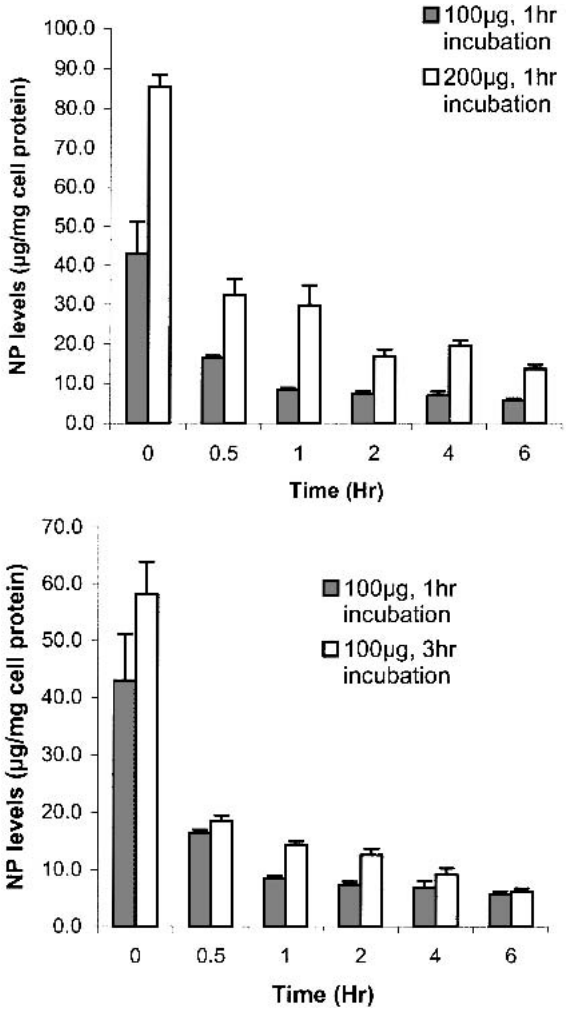

Fig. 5. Effect of nanoparticle (NP) dose (A) and preincubation time (B) on nanoparticle exocytosis. Vascular smooth muscle cells were incubated with nanoparticles for the time indicated, washed and incubated with fresh medium (0 h time point). Medium was removed and cells were washed and analyzed for nanoparticle levels at different time points. Data as mean ± SEM, n = 4.

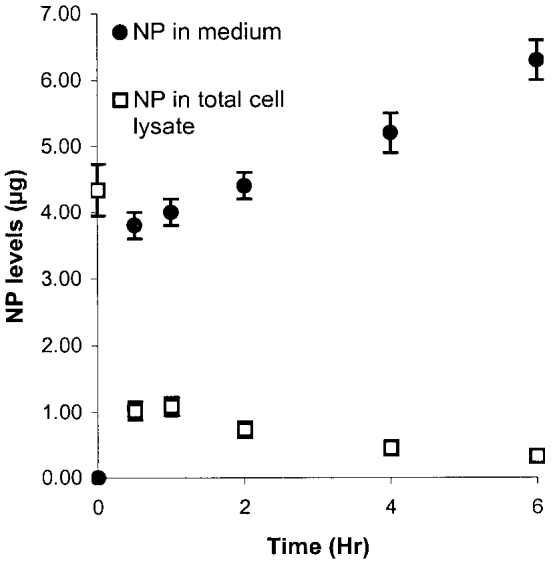

Fig. 6. Mass balance in nanoparticle exocytosis from vascular smooth muscle cells. Vascular smooth muscle cells were incubated with nanoparticles (100 µg/mL) for 1 h, washed, and incubated with fresh medium (0 h time point). Nanoparticle levels in both the medium and the total cell lysate were analyzed at different time points. Data as mean ± SEM, n = 4.

els dropped to about 10% of its 0 h value within about 30 min and remained constant thereafter, whereas for PLGA nanoparticles a higher fraction was retained intracellularly at 30 min (~35%) and 15% at the end of 6 h for 100 µg/mL dose. Exocytosis of nanoparticles was decreased in the presence of metabolic inhibitors, sodium azide and deoxyglucose. Metabolic inhibition did not affect the initial drop in nanoparticle levels during the first 1 h. This was expected because previous studies have shown that preincubation for at least 1 h is necessary for the metabolic inhibitors to inhibit cell processes (5). However, the exocytosis of nanoparticles was partially inhibited thereafter and was reduced by about 40% as compared with respective controls (without metabolic inhibitors) at the end of 6 h, suggesting that exocytosis is an active process (Fig. 7B).

The exocytosis of nanoparticles was inhibited almost completely when the endocytosis and exocytosis were carried out in the serum free medium (Fig. 8). Addition of 1% BSA in the serum-free medium resulted in the exocytosis of nanoparticles similar to the exocytosis observed in serum containing medium (Fig. 9). Addition of platelet derived growth factor (PDGF) along with 1% BSA did not show any additional effect on exocytosis of nanoparticles (Fig. 9).

DISCUSSION

Nanoparticles formulated from PLGA polymer offer a nontoxic and efficient carrier system for the sustained intracellular delivery of different therapeutic agents (10). However, the advantages of PLGA nanoparticles might be offset if they are not retained within the cells, especially when intracellular delivery of therapeutic agents is desired. Hence, in the current study, we characterized the uptake and retention of PLGA nanoparticles in an *in vitro* cell culture model. Nanoparticles were internalized efficiently by VSMCs and the uptake was concentration- and time-dependent. A decrease in the efficiency of nanoparticle uptake at higher doses and after prolonged incubation suggests that the cellular nanoparticle uptake pathway is saturable. Furthermore, the partial inhibition in nanoparticle uptake after energy depletion suggests an endocytic uptake process (16). Uptake of particulate systems could occur through various processes, such as by phagocytosis, fluid phase pinocytosis, or by receptor-mediated endocytosis (17,18). Phagocytosis is the main mechanism by which particulate systems are internalized by macrophages (17). VSMCs are also known to be phagocytic, actively phagocytosing other apoptotic VSMCs (19). However, using a phagocytosis kit (Fc-OxyBurst™, Molecular Probes), we did not detect any phagocytic activity in the presence of nanoparticles. A possible reason for the above phenomenon could be the fact that our nanoparticles are ~100 nm, which is smaller than the 500 nm lower size cut-off described for phagocytosis (20).

It has been previously suggested that a linear uptake process is an indicative of fluid phase pinocytosis whereas saturable uptake is an indicative of receptor-mediated uptake (21). Because the uptake of nanoparticles is concentration

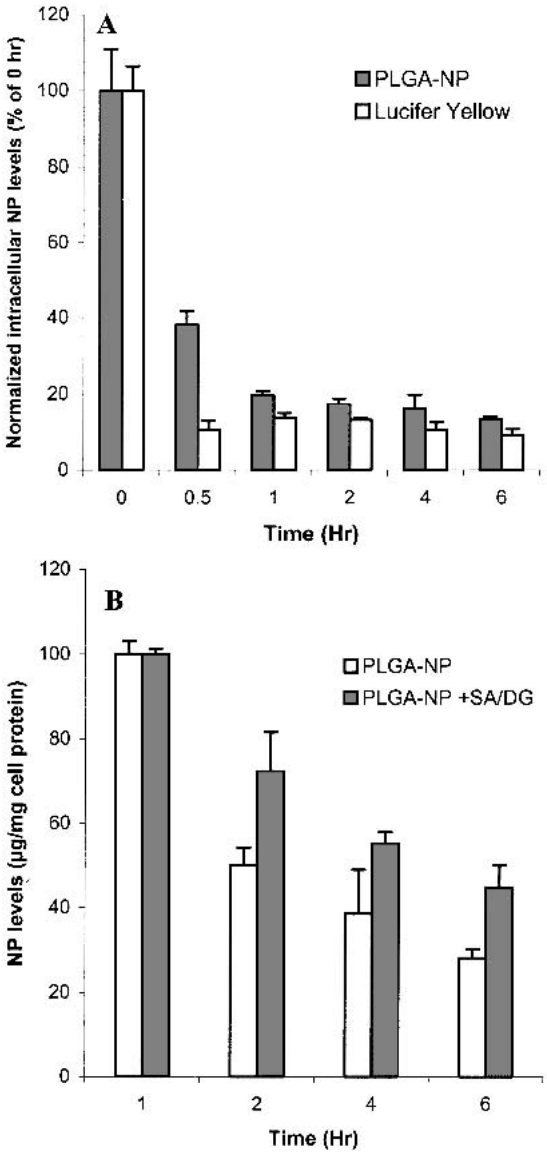

Fig. 7. (A) Exocytosis of fluid phase marker, Lucifer yellow, from vascular smooth muscle cells (VSMCs) compared with nanoparticles (PLGA-NP, 100 µg/mL). VSMCs were incubated with nanoparticles or Lucifer yellow for 1 h, washed, and incubated with fresh medium (0 h time point). The medium was removed and cells were washed and analyzed for either lucifer yellow or nanoparticle levels at different time points. (B) Effect of metabolic inhibitors (sodium azide + deoxyglucose) on exocytosis of nanoparticles. VSMCs were incubated with nanoparticles (100 µg/mL) for 1 h, washed, and incubated with fresh medium with (PLGA-NP+SA/DG) or without (PLGA-NP) sodium azide and deoxyglucose. Medium was removed and cells were washed and analyzed for nanoparticle levels at different time points. Nanoparticle levels at 1 h, which were similar for both the groups, were taken as 100% to compare the relative exocytosis at later time points. There was no significant difference in the exocytosis rate and extent during the first 1 h. Data as mean ± SEM, n = 4.

dependent at a lower concentration range, it could suggest that the nanoparticle uptake is by fluid phase pinocytosis. At higher concentrations of nanoparticles, the cells probably reached a saturation uptake, and hence the uptake efficiency is reduced. Also, we have previously demonstrated that inhibition of clathrin-coated pits (and not of caveoli), which in

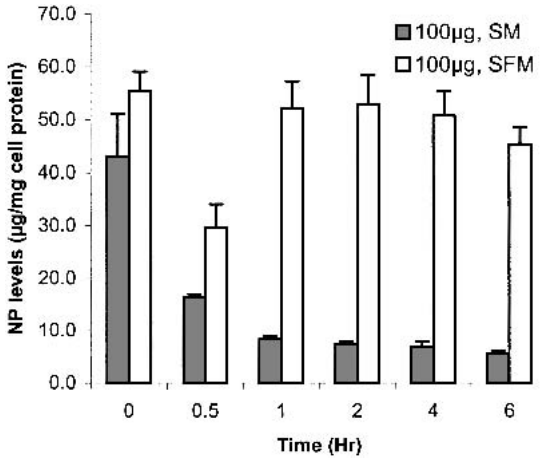

Fig. 8. Effect of serum on nanoparticle (NP) exocytosis. Vascular smooth muscle cells were incubated with nanoparticles for 1 h, washed, and incubated with fresh medium (0 h time point). Medium was removed and cells were washed and analyzed for nanoparticle levels at different time points. SM, serum containing medium; SFM, serum-free medium. Data as mean ± SEM, n = 6.

turn inhibits receptor-mediated endocytosis, results in only about 40% inhibition of nanoparticle uptake (5). Thus, nanoparticles could be transported in part through nonspecific receptor mediated endocytosis and in part through fluid-phase endocytosis.

Intracellular levels of nanoparticles increased when the concentration of nanoparticles was maintained in the extracellular medium. However, when the nanoparticle suspension was replaced with fresh medium, intracellular levels of nanoparticles decreased. Exocytosis of nanoparticles was an active process, as suggested by its energy dependence. Overall, the results suggest that nanoparticle endocytosis and exocytosis

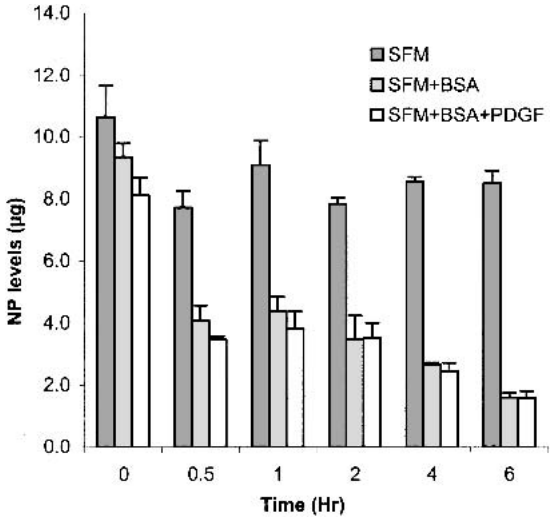

Fig. 9. Effect of BSA and PDGF on the exocytosis of nanoparticles in serum-free medium (SFM). Vascular smooth muscle cells were incubated with nanoparticles (200 µg/mL) for 1 h, washed, and incubated with fresh medium (0 h time point). Medium was removed and cells were washed and analyzed for nanoparticle levels at different time points. Nanoparticle (NP) uptake was not normalized to cell protein in this experiment due to adsorption of BSA to cell surface resulting in higher total cell protein values. Data as mean ± SEM, n = 6.

are dynamic and energy-dependent processes, with both endocytosis and exocytosis proceeding simultaneously. It has been previously reported that in rat adipocytes, about 110,000 endocytic vesicles of approximately 100 nm in diameter are formed per cell per hour and results in 20% of the plasma membrane of the cell being recycled per hour (22). The internalized membranes are replaced by exocytic vesicles at the same rate as the internalization rate. Thus, when the nanoparticles are present in the external medium, there would be a constant recycling of a fraction of nanoparticles into and out of the cell. At any point in time, the amount of nanoparticles inside the cell would be represented by the nanoparticles that are in the process of recycling inside the cell, the fraction that is in the lysosomes and the fraction that has escaped into the cytoplasm (5). Once the nanoparticles are removed from the external medium, concentration of nanoparticles outside the cell drops, and the recycling is disturbed, resulting in a drop in intracellular nanoparticle levels. The biphasic drop in the intracellular nanoparticle levels suggest that at least two intracellular compartments could be involved: the first, which turns over rapidly, and the second, which turns over relatively slowly (23). Although not investigated in this study, it is possible that the recycling endosomes represent the fast turn over compartment (24) and the fraction of nanoparticles that escaped the recycling endosomes either into cytoplasmic compartment or transported to the lysosomes could represent nanoparticles in the second slow turn over compartment (25). Recycling of particulate carrier systems has been known and is reported for liposomes (26). It was previously suggested that there are two possible compartments for exocytosis of fluid phase markers such as Lucifer yellow; one small and turning over rapidly, and another apparently larger one (presumably lysosomes) which fills and empties slowly (25). The above phenomenon may also explain the increase in the amount of nanoparticles retained intracellularly with the increase in the dose of nanoparticles. It could have been due to the increase in the amount of nanoparticles escaping into the cytoplasm or those transported to the lysosomes.

Exocytosis of fluid phase marker was faster when compared with the exocytosis of nanoparticles. A major amount of the fluid phase marker is probably trapped at the level of the rapid recycling compartment and is available for immediate export from the cell. Thus, about 90% of the internalized fluid phase marker is exocytosed within 30 min of removal of the medium (Fig. 7A). The differences in the exocytosis rate between nanoparticles and Lucifer yellow could be attributed to the differences in their size and nature. Size of the fluid phase marker affects the transfer of the marker from the fast recycling compartment to the slow recycling compartment and also the rate of recycling from the slow recycling compartment (25,27). Thus, it was previously demonstrated that a majority of the internalized Lucifer yellow (molecular weight ~450) was trapped at the level of rapid recycling compartment (25) whereas for larger molecular weight marker, horseradish peroxidase (molecular weight ~40,000), a greater fraction of the internalized marker enters the slow recycling compartment, resulting in slower exocytosis (27). It is also further suggested that the rate of exocytosis from the slower recycling compartment (lysosomes) is dependent on molecular weight of the internalized solute and may be limited by the rate of diffusion of molecules into shuttle vesicles (27). Thus, nanoparticles, with a lower diffusion coefficient compared to Lucifer yellow or other soluble markers because of their particulate nature, would be expected to show a slower rate of exocytosis. It is also possible that the nanoparticles localized in the cytoplasmic compartment may be slow in diffusing across the cell membrane for exocytosis because of the gel-like viscous characteristics of the cytoplasmic fluid.

Interestingly, the exocytosis of nanoparticles was inhibited in serum-free medium. To clarify the role of serum in inducing nanoparticle exocytosis, we studied the effect of BSA and a growth factor (PDGF) because the main components of serum include albumin and growth factors. Addition of 1% BSA to the serum-free medium resulted in complete restoration of exocytosis, suggesting that albumin induces exocytosis. It has been previously reported that BSA in the medium is actively endocytosed and that the endosomes containing the newly internalized BSA can interact with the exocytosis pathway (28). Accordingly, BSA has been shown to increase the exocytosis of the nondegradable tracer poly-D-lysine in rabbit alveolar macrophages (28). The addition of PDGF, a potent mitogen for VSMCs, in the BSA solution did not affect the nanoparticle exocytosis (Fig. 9). Furthermore, it was observed that serum in the medium does not affect the uptake of nanoparticles, suggesting the predominant role of the serum in the process of exocytosis of nanoparticles. For a number of cationic lipids/polymers and other commercially available transfecting agents, transfection experiments are conducted in serum-free medium, and it is suggested that reduction in the uptake of these agents in the presence of serum could lead to the loss in their activity (29). Our report suggests that exocytosis of these DNA-transfecting reagent complexes in the presence of serum could also be one of the possible causes for the loss of their transfectivity in serum-containing medium.

Although the drop in intracellular nanoparticle levels could lead to lower efficiency of nanoparticle-mediated intracellular drug delivery, it has to be realized that the nanoparticle concentration outside the cell may not fall so rapidly *in vivo*. It has been previously demonstrated that when the nanoparticles are delivered locally into the vascular tissue, the drug levels in the tissue are sustained for at least up to 7–14 days (30,31). Thus, *in vivo*, there could be a constant presence of nanoparticles next to or near the cells, which might lead to mass transport equilibrium being reached, resulting in higher intracellular nanoparticle levels. Also, exocytosis of nanoparticles taken up by the endothelial cells could result in nanoparticle-entrapped drug reaching to more distant VSMC populations. Further, the sustained antiproliferative effect (~2 weeks) observed in our previous studies with a single-dose of dexamethasone-loaded nanoparticles *in vitro* in VSMCs as compared to the transient effect (~3 days) of an equivalent dose of dexamethasone in solution, suggests that a fraction of nanoparticles retained intracellularly results in the prolonged therapeutic effect of the encapsulated drug (5). Furthermore, in previous studies, we have demonstrated inhibition of restenosis in a rat carotid artery model with single-dose localized intraluminal delivery of dexamethasone-loaded nanoparticles, suggesting sustained antiproliferative effect of the nanoparticle-encapsulated therapeutic agent *in vivo* (31). Although the dynamics of endocytosis and exocytosis *in vivo* could be different from that observed *in vitro*, it is important to understand the factors affecting the cellular uptake of

nanoparticles, and their intracellular trafficking and sorting mechanisms to further explore the drug delivery applications of nanoparticles.

From a mechanistic point of view, the results from our previous (5) and current studies suggest that nanoparticles are taken up by VSMCs by an energy-dependent endocytic process involving fluid-phase pinocytosis and nonspecific receptor-mediated endocytosis. After their uptake, a fraction of nanoparticles recycle back to the outside of the cell, whereas another fraction enters secondary endosomes and lysosomes. Some of the nanoparticles escape into the cytoplasm from the endo-lysosomes. From the above results, it could be speculated that there are two potential barriers to the cytoplasmic escape of nanoparticles: first, the transport of nanoparticles from fast recycling compartment to the endo-lysosomes; and second, the escape of nanoparticles from endo-lysosomes. Our previous studies suggest that reversal of a nanoparticle's surface charge in the acidic pH of the endo-lysosomes is responsible for their endo-lysosomal escape (5). However, it is not known as to what factors affect the transport of nanoparticles from recycling compartment to the endo-lysosomes or what fraction of nanoparticles escape the endo-lysosomal compartment into the cytoplasm. Our current efforts are directed at investigating these aspects and formulating nanoparticles that will have a higher intracellular uptake and retention, with the objective of achieving higher and longer intracellular retention of the entrapped therapeutic agent. It would be interesting to determine how the dynamics of endocytosis and exocytosis changes for ligand-conjugated nanoparticles whose uptake is mediated via specific receptors. Furumoto *et al.* (32) have reported that exocytosis of polystyrene nanoparticles in hepatocytes was much lower when the particle uptake was mediated by apo-E than via asialoglycoprotein receptor, suggesting that ligand-conjugated nanoparticles could have different intracellular sorting mechanism than unconjugated nanoparticles, which in turn could affect their uptake and retention.

CONCLUSIONS

We have characterized the intracellular uptake and retention of nanoparticles in VSMCs. Nanoparticles were internalized rapidly and efficiently by an energy-dependent process that was saturable. Exocytosis of a major fraction of internalized nanoparticles occurred rapidly once the nanoparticles in the external medium were removed. Exocytosis was dependent on the dose of nanoparticles and on the presence of BSA in the medium. A better understanding of the mechanisms of endocytosis and exocytosis, studies determining the effect of nanoparticle formulation and composition that may affect both the processes, and characterization of intracellular distribution of nanoparticles with surface modifications would be useful in exploring nanoparticles for intracellular delivery of therapeutic agents.

ACKNOWLEDGMENTS

Funding for the project from the National Institutes of Health, Heart, Lung and Blood Institute (HL 57234) and the Nebraska Research Initiative-Gene Therapy Program. A predoctoral fellowship to JP from the American Heart Association, Heartland Affiliate. We would like to thank Janice Taylor of the confocal laser microscopy core facility at UNMC for her assistance with the microscopic studies and Elaine Payne for providing administrative assistance.

REFERENCES

1. F. Liu and L. Huang. Development of non-viral vectors for systemic gene delivery. *J. Control. Release* **78**:259–262 (2002).
2. M. C. Morris, J. Depollier, J. Mery, F. Heitz, and G. Divita. A peptide carrier for the biologically active proteins into mammalian cells. *Nat. Biotechnol.* **19**:1173–1176 (2001).
3. S. R. Schwarze and S. F. Dowdy. In vivo protein transduction: Intracellular delivery of biologically active proteins, compounds and DNA. *Trends Pharmacol. Sci.* **21**:45–48 (2000).
4. H. Riezman, P. G. Woodman, G. van Meer, and M. Marsh. Molecular mechanisms of endocytosis. *Cell* **91**:731–738 (1997).
5. J. Panyam, W. Z. Zhou, S. Prabha, S. K. Sahoo, and V. Labhasetwar. Rapid endo-lysosomal escape of poly (D,L-lactide-co-glycolide) nanoparticles: Implications for drug and gene delivery. *FASEB J.* **16**:1217–1226 (2002).
6. S. Prabha, W. Z. Zhou, J. Panyam, and V. Labhasetwar. Size-dependency of nanoparticle-mediated gene transfection: Studies with fractionated nanoparticles. *Int. J. Pharm.* **244**:105–115 (2002).
7. S. K. Sahoo, J. Panyam, S. Prabha, and V. Labhasetwar. Residual polyvinyl alcohol associated with poly (D, L-lactide-co-glycolide) nanoparticles affects their physical properties and cellular uptake. *J. Control. Release* **82**:105–114 (2002).
8. J. M. Anderson and M. S. Shive. Biodegradation and biocompatibility of PLA and PLGA microspheres. *Adv. Drug Deliv. Rev.* **28**:5–24 (1997).
9. V. Labhasetwar. Nanoparticles for drug delivery. *Pharm. News* **4**:28–31 (1997).
10. J. Panyam and V. Labhasetwar. Biodegradable nanoparticles for drug and gene delivery to cells and tissue. *Adv. Drug Del. Rev.* (2002) in press.
11. V. Labhasetwar, C. Song, and R. J. Levy. Nanoparticle drug delivery for restenosis. *Adv. Drug Deliv. Rev.* **24**:63–85 (1997).
12. V. Labhasetwar, C. Song, W. Humphrey, R. Shebuski, and R. J. Levy. Arterial uptake of biodegradable nanoparticles: Effect of surface modifications. *J. Pharm. Sci.* **87**:1229–1234 (1998).
13. E. R. O'Brien, C. E. Alpers, D. K. Stewart, M. Ferguson, N. Tran, D. Gordon, E. P. Benditt, T. Hinohara, J. B. Simpson, and S. M. Schwartz. Proliferation in primary and restenotic coronary atherectomy tissue. Implications for antiproliferative therapy. *Circ. Res.* **73**:223–231 (1993).
14. J. Davda and V. Labhasetwar. Characterization of nanoparticle uptake by endothelial cells. *Int. J. Pharm.* **233**:51–59 (2002).
15. J. Panyam, J. Lof, E. O'Leary, and V. Labhasetwar. Efficiency of Dispatch® and Infiltrator® cardiac infusion catheters in arterial localization of nanoparticles in a porcine coronary model of restenosis. *J. Drug Target.* **10**:515–523 (2002).
16. V. P. Torchilin, R. Rammohan, V. Weissig, and T. S. Levchenko. TAT peptide on the surface of liposomes affords their efficient intracellular delivery even at low temperature and in the presence of metabolic inhibitors. *Proc. Natl. Acad. Sci. USA* **98**:8786–8791 (2001).
17. K. A. Foster, M. Yazdanian, and K. L. Audus. Microparticulate uptake mechanisms of in-vitro cell culture models of the respiratory epithelium. *J. Pharm. Pharmacol.* **53**:57–66 (2001).
18. H. Suh, B. Jeong, F. Liu, and S. W. Kim. Cellular uptake study of biodegradable nanoparticles in vascular smooth muscle cells. *Pharm. Res.* **15**:1495–1498 (1998).
19. M. R. Bennet, D. F. Gibson, S. M. Schwartz, and J. F. Tait. Binding and phagocytosis of apoptotic vascular smooth muscle cells is mediated in part by exposure of phosphatidylserine. *Circ. Res.* **77**:1136–1142 (1995).
20. A. Rupper and J. Cardelli. Regulation of phagocytosis and endophagosomal trafficking pathways in Dictyostelium discoideum. *Biochim. Biophys. Acta* **1525**:205–216 (2001).
21. A. Catizone, A. L. Medolago Albani, F. Reola, and T. Alescio. A quantitative assessment of non specific pinocytosis by human endothelial cells surviving in vitro. *Cell Mol. Biol.* **39**:155–169 (1993).

22. E. M. Gibbs and G. E. Lienhard. Fluid-phase endocytosis by isolated rat adipocytes. *J. Cell. Physiol.* **121**:569–575 (1984).
23. B. Goud, C. Jouanne, and J. C. Antoine. Reversible pinocytosis of horse radish peroxidase in lymphoid cells. *Exp. Cell Res.* **153**: 218–235 (1984).
24. J. Gruenberg. The endocytic pathway: a mosaic of domains. *Nat. Rev. Mol. Cell Biol.* **2**:721–730 (2001).
25. J. A. Swanson, B. D. Yirinec, and S. C. Silverstein. Phorbol esters and horseradish peroxidase stimulate pinocytosis and redirect the flow of pinocytosed fluid in macrophages. *J. Cell Biol.* **100**:851–859 (1985).
26. M. Colin, M. Maurice, G. Trugnan, M. Kornprobst, H. R.P., A. Knight, R. G. Cooper, A. D. Miller, J. Capeau, C. Coutelle, and M. C. Brahimi-Horn. Cell delivery, intracellular trafficking and expression of an integrin-mediated gene transfer vector in tracheal epithelial cells. *Gene Ther.* **7**:139–152 (2000).
27. M. J. Buckmaster, D. Lo Braico Jr., A. L. Ferris, and B. Storrie. Retention of pinocytized solute by CHO cell lysosomes correlates with molecular weight. *Cell Biol. Int. Rep.* **11**:501–507 (1987).
28. H. Tomoda, Y. Kishimoto, and Y. C. Lee. Temperature effect on endocytosis and exocytosis by rabbit alveolar macrophages. *J. Biol. Chem.* **264**:15445–15450 (1989).
29. M. Teresa Girao da Cruz, S. Simoes, P. P. C. Pires, S. Nir, and M. C. Pedroso de Lima. Kinetic analysis of the initial steps involved in lipoplex-cell interactions: Effect of various factors that influence transfection activity. *Biochim. Biophys. Acta* **1510**:136–151 (2001).
30. I. Fishbein, M. Chorny, S. Banai, A. Levitzki, H. D. Danenberg, J. Gao, X. Chen, E. Moerman, I. Gati, V. Goldwasser, and G. Golomb. Formulation and delivery mode affect disposition and activity of tryphostin-loaded nanoparticles in the rat carotid model. *Arterioscler. Thromb. Vasc. Biol.* **21**:1434–1439 (2001).
31. L. A. Guzman, V. Labhasetwar, C. Song, Y. Jang, A. M. Lincoff, R. Levy, and E. J. Topol. Local intraluminal infusion of biodegradable polymeric nanoparticles. A novel approach for prolonged drug delivery after balloon angioplasty. *Circulation* **94**: 1441–1448 (1996).
32. K. Furumoto, K. Ogawara, M. Yoshida, Y. Takakura, M. Hashida, K. Higaki, and T. Kimura. Biliary excretion of polystyrene microspheres depends on the type of receptor-mediated uptake in rat liver. *Biochim. Biophys. Acta* **1526**:221–226 (2001).